An Annealed Polyelectrolyte Brush in a Polar−Nonpolar Binary Solvent: Effect of pH and Ionic Strength

A. A. Mercurieva,[†] T. M. Birshtein,[†] E. B. Zhulina,[†] P. Iakovlev,[†] J. van Male,[‡] and F. A. M. Leermakers*[,‡]

Institute of Macromolecular Compounds of the Russian Academy of Sciences, 199004, St. Petersburg, Russia, and Laboratory of Physical Chemistry and Colloid Science, Wageningen University, Dreijenplein 6, 6703 HB Wageningen, The Netherlands

Received October 30, 2001; Revised Manuscript Received March 21, 2002

ABSTRACT: A weakly charged polyelectrolyte brush in a polar−nonpolar solvent mixture is studied using a boxlike model and by numerical self-consistent-field theory. The work is a continuation of a similar study of a neutral polymer brush in a solvent mixture with a pronounced solubility gap. We study both the structure and structural transitions of the brush in particular in the one-phase region of the solvent mixture in the bulk. With respect to the neutral system, the polyelectrolyte system is even richer in its behavior. Starting from a nonpolar main solvent, upon increasing the chemical potential of water, we find the development of a mesoscopic water film inside the brush. The polymer takes up this thin film as it finds an environment that allows for the dissociation of its groups energetically attractive. The phase transition can be accompanied by an anomalous collapse of the ionizable brush and tuned by the pH of the solution and the ionic strength in the system. Another brush transition can occur when nonpolar solvent is added to a brush immersed in water. Finally, it is feasible that systems exist that feature three successive brush transitions upon changing the bulk composition from pre-binodal, to biphasic, and then to post-binodal compositions, where a forward, a reentry, and again a forward transition are found, respectively.

1. Introduction

The polymer brush continues to be a structure that receives warm interest from the polymer physics community.[1−4] After some pioneering years of polymer brush theory and experimental work in this area, there is now good evidence that end-grafted polymers at interfaces have unique properties. When the chains are planted at high enough density, the chains are strongly stretched. The thickness of the brush, also called the height of the brush, is proportional to the chain length, and in many cases the end points of the brush chains remain distributed throughout the layer. This last result indicates that there are anomalously large fluctuations present. Polymer brushes have interesting applications. They may be used to protect surfaces from contaminations (antifouling agents). Other applications can make use of the soft character of these interfaces, e.g., in cell adhesion or vesicle adhesion surfaces. Polymer brushes may be used to influence the colloidal stability[5] of particles in solution and as such may have huge impact in many engineering applications. When particles are immersed in binary solvent mixtures that are not fully miscible, one can have the possibility that three faces come together. Then, one can use polymer brushes to tune the wettability of surfaces. Closely related to these systems are applications in the field of polymer chromatography.

In this paper we pick up issues related to the polymer aspect of the problem. Recently, some work was done on the behavior of a polymer brush in a binary solvent, both from a polymer and from a wetting perspective.[6−14] In particular, the case that the solvent has a large solubility gap was selected (cf. Figure 1). The behavior of a brush under these conditions is very special. It was found that when the polymer molecules were able to dissolve about equally well in the two solvents, but in particular, when it dissolves slightly better in the wetting solvent, a first-order transition can occur where there is a jump in the conformational characteristics of the polymers.[12−14] This jump occurs when the solvent mixture is still in the one-phase region, not too far from

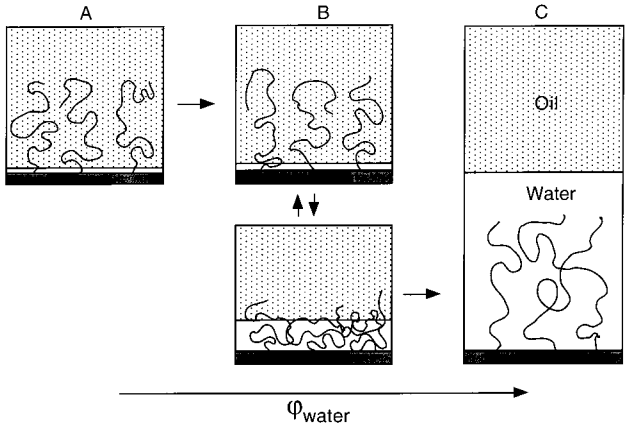

Figure 1. Schematic representation of the structures of a (neutral) amphiphilic polymer brush in a binary mixture of solvents (oil = gray scaling on top; water = phase near surface). (A) The water concentration is very low; the polymer is stetched in the oil (reasonably good solvent) phase. (B) The water concentration is close to, but below, the saturation value; here a first-order phase transition takes place where the water film grows stepwise from a microscopic to a mesoscopic thickness, and the polymer collapses into this water film. (C) The water concentration reaches the binodal value; the water film grows to macroscopic size, and the brush is again swollen (water is very good solvent). In contrast to this system, the polymer chains in the present study are charged. Details are in the text.

[†] Institute of Macromolecular Compounds of the Russian Academy of Sciences.
[‡] Wageningen University.

10.1021/ma011884p CCC: $22.00
Published on Web 05/10/2002

the binodal value and is shown in Figure 1B where the top brush is in equilibrium with the lower brush. In this case a wetting film of the minority solvent develops in the brush near the interface. The wetting film remains necessarily of mesoscopic size because the system is still off-coexistence. Then, because the polymer has some affinity for the wetting component, it tends to be in this thin film of good solvent. By doing so, it collapses in the sense that the thickness of the brush suddenly strongly reduces. This transition has been found in ref 12 by an investigation along the lines of the Alexander−de Gennes box model[1,15] that has been complemented in refs 13 and 14 by a more exact numerical analysis of the self-consistent-field (SCF) equations[16−21] carried out in the approximations elaborated by Scheutjens and Fleer.[22] This strategy proved to be very reasonable: the box model captures many of the important features of the system.

One of the problems of previous studies was that the parameters necessary to observe these anomalous features are such that one could argue that only rather special experimental systems can meet all necessary requirements. For example, as suggested in Figure 1A,C, the brush should be swollen both in the oil (A) and in the water (C) phase. This type of amphiphilicity may be very difficult to generate with neutral polymer systems. However, it was already suggested that very likely these conditions could be found in a polyelectrolyte system and especially in weak polyelectrolytes where ionized and hydrophobic groups are distributed along the chain more or less equally. Of course, these polyelectrolytes are only marginally soluble in water if they are uncharged. In such a system a useful wetting component is water. When the polyelectrolyte molecules are in water, they can be ionized (annealed polyelectrolytes[23,24]). The degree of their ionization depends on the pH and on the ionic strength of the solution. On the other hand, in organic solvents the "hydrophobic" polyelectrolytes are very weakly charged and remain in good solvent. In principle, this dualistic behavior (cf. Figure 1) opens up interesting issues, and we will come to some of them below in detail.

The theoretical investigation of the system is constructed by applying two models. The first one is the most simplified box model, wherein the brush is considered homogeneous both in the lateral and in the normal (to the grafting surface) direction. The second one is a more exact SCF theory. In this case only the lateral homogeneity assumption is left, and the change of brush structure with its height becomes one of the observables. Clearly, the lateral homogeneity of a *swollen* polymer brushes is completely justified, and as we will show, the use of the more simplified box models is also surprisingly accurate. However, as we will also see, it is possible to observed a *collapse* of the brush. In principle, such a collapsed structure may lead to heterogeneity in all directions, in which case also the SCF model is too approximate. We will return to the aspect of the adaptability of the applied theories for laterally homogeneous models to the real systems in the Experimental Aspects section.

The remainder of this paper is the following. First, we will describe a proper modification of the box model[1,15] for annealed polyelectrolytes in a binary mixture, with pH and ionic strength as variables. We will combine the introduction of the essential equations with the specifications of the model for both salt-free and salt-added systems. In the subsequent subsection we will briefly outline the numerical SCF theory for the considered system giving only the necessary points. (A paper with detailed background information on the SCF aspects will be published elsewhere.) In the following subsection the chosen set of parameters will be introduced. The second part will contain the results of the calculations. We will begin with the results of the calculations in the framework of the box model. Then the results of the numerical SCF calculations will be compared with those presented for the box model. A good agreement between the models will be demonstrated, and additional information gained from the SCF calculations will be discussed. Some experimental aspects are discussed just before the main conclusions are summarized.

2. General Formalism

A. Model and Notations. We consider a laterally homogeneous polymer brush composed of long polymer chains grafted at the density $1/\sigma$ (σ is area per chain). The chains consist of N symmetrical monomers of size a. As usual, all linear dimensions are expressed in these a units. The brush is immersed into a mixture of highly incompatible solvents referred below as a generic nonpolar solvent B and a polar admixture (water). The reversed case, i.e., that the water is the main solvent and the nonpolar solvent is the minority solvent, will receive some attention at the end of this paper. The polymer is a weak polyacid HA capable of ionization in particular when it is immersed into water. The dissociation reaction in water

$$HA + H_2O \leftrightarrow A^- + H_3O^+ \qquad (1)$$

is parametrized by the reaction constant K. The degree of dissociation is given by α. Water itself dissociates; the reaction is

$$2H_2O \leftrightarrow OH^- + H_3O^+ \qquad (2)$$

We assign the constant K_W to this reaction. The concentration of H_3O^+ ions is equivalent to the concentration of protons, which, in turn, specifies the pH.

Hence, the system under consideration involves six components, namely, neutral and charged polymer segments, solvent B, water, OH^- and H_3O^+ ions. If salt (NaCl, for example) is present, Na^+ and Cl^- ions also contribute to the thermodynamics, and the system has eight components. For simplicity, we assume all monomeric components to be symmetrical and of equal molecular volume. The incompressibility constraint is supposed to be fulfilled:

$$\sum_J \varphi_J(z) = 1 \qquad (3)$$

Here ϕ_J is a volume fraction of the Jth species, while z corresponds to the number of the lattice layer in the brush. It is important to mention that in the box model ϕ_J is supposed to be independent of z.

The variety of components results in a variety of interactions. The interaction between the two solvents is characterized by the Flory−Huggins parameter χ_{BW}. Note that incompatibility appears when $\chi_{BW} > 2$. The nonelectrostatic interactions of the polymer units with the solvent B and water are also described by the usual

Flory−Huggins parameters, χ_B and χ_W, respectively. The polymer−water interactions are assumed to be the same whether the polymer segments and the water molecules are ionized or not. Moreover, if the salt ions are present, their nonelectrostatic interactions with the polymer segments are also described by the value χ_W adopted for the polymer−water interactions. Note that, under the conditions considered in this paper (low values of the salt concentration and, as a result, the osmotic regime of the polyelectrolyte brush behavior[23−26]), the brush contains virtually only counterions H_3O^+ or Na^+, and thus interactions involving co-ions and respective parameters are not essential.

A part of electrostatic interactions pertains to interactions of mobile ions with bound charges of the brush. We discuss these interactions in detail later since they are considered distinctly in the box and the SCF models. Another part of electrostatic interactions is mimicked by introducing the χ_{Be} parameter for interactions of the solvent B with charged groups.[27] We assume it to be the same for all charged groups, i.e., ionized polymer segments, ions of water and salt. As is shown below, at $\chi_{Be} > 0$, the polymer ionization is suppressed by the solvent B. This is manifested by a decrease in the effective disscociation constant for the polymer units.

B. Box Model. 1. Salt-Free System. The brush forms a layer of the thickness H, and in the volume $H\sigma$ one finds $n_p = N$ of the polymer segments and n_B and n_W molecules of the solvent B and water. The polymer segments HA dissociate, the degree of dissociation is given by α, and the number of protons dissociated from the polymer is $n_p\alpha$. Here we consider a salt-free system and assume that all counterions remain inside the brush due to electrostatic interactions. Following the well-known terminology proposed in refs 25 and 26, this corresponds to the OsB regime. We also assume that there are no co-ions inside the brush. The net charge of protons is equal in magnitude but opposite to the net polymer charge. This is an electroneutrality condition and, moreover, a local electroneutrality condition. Therefore, the number of the polymer segments, molecules of the solvent B, water H_2O, and protonated water H_3O^+ in the volume $H\sigma$ totals $n_p(1 + \alpha) + n_B + n_W$. The corresponding volume fractions are given by $\phi_x = n_x/H\sigma$ (x = p, B, W) and connected by the relation akin to eq 3, namely:

$$\phi_B + \phi_W + \phi_p(1 + \alpha) = 1 \tag{4}$$

The dimensionless free energy of the brush (per polymer segment) in the solvent mixed of the two components, nonpolar B and water, in the case of dissociation is given by

$$\Delta F^{in} = \frac{H^2}{n_p^2} + \left[\frac{n_B}{n_p}\ln \varphi_B + \frac{n_W}{n_p}\ln \varphi_W + \alpha \ln \alpha\varphi_p + \alpha \ln \alpha + (1-\alpha)\ln(1-\alpha)\right] + \left[\frac{n_B}{n_p}(\chi_B(1-\alpha)\varphi_p + 2\chi_{Be}\alpha\varphi_p + \chi_{BW}\varphi_W) + \chi_W\left(\frac{n_W}{n_p} + \alpha\right)\varphi_p\right] + \Delta\mu\alpha \tag{5}$$

We use dimensionless parameters; all energies are scaled by the temperature k_BT. Unimportant numerical factors of the order of unity are neglected. The conformational free energy of the brush is written in its standard Gaussian form, H^2/N. The terms enclosed in the first square brackets give the mixing entropy of the components including mixing of ionized and nonionized polymer segments and protonated water molecules. The second square brackets contain terms describing interactions between the components in the system in the usual Flory−Huggins approximation. The term proportional to $\Delta\mu$ accounts for the contribution of the dissociation (eq 1) and is directly related to the reaction constant K by the equation $K = \exp(-\Delta\mu)$.

Since all mobile counterions are produced by the polymer ionization, the degree of polymer dissociation α is just determined by the free energy of the brush itself. Minimization of the free energy given by eq 5 with respect to α enables us to find the following equation for an equilibrium value of the degree of polymer dissociation:

$$\frac{\alpha^2\varphi_p}{1-\alpha} = \varphi_W\tilde{K}^0 \tag{6}$$

Here $\tilde{K}^0$ is introduced which is given by

$$\tilde{K}^0 = K\exp(-\varphi_B(2\chi_{Be} - \chi_B - \chi_{BW})) \tag{7}$$

This parameter is an analogue of the dissociation constant K and includes the effects of the presence of the solvent B in the mixture. Evidently, $\tilde{K}^0$ decreases as the concentration of the solvent B inside the brush increases.

With $\tilde{K}^0$ instead of K, eq 6 is completely identical to that obtained previously[23] for ionization of a polyacid brush in water (OsB regime). It accounts for the fact that with a rise in α the concentration of protons in the solvent inside the brush, i.e., its acidity, also increases, which, in turn, blocks further ionization.

Substitution of eqs 6 and 7 into eq 5 gives ΔF^{in} at the equilibrium value of the degree of ionization α:

$$\Delta F^{in} = \frac{H^2}{n_p^2} + \frac{\varphi_B}{\varphi_p}\ln \varphi_B + \varphi_B\chi_B + \frac{1-\varphi_p-\varphi_B}{\varphi_p}(\ln \varphi_W + \varphi_p\chi_W + \varphi_B\chi_{BW}) + \ln(1-\alpha) \tag{8}$$

It is notable that this relation includes only three χ parameters, namely χ_B, χ_W, and χ_{BW}, accounting for the nonelectrostatic interactions, whereas a standard term $\ln(1 - \alpha)$ is taking care of all effects of ionization and electrostatic interactions.

Equation 8 together with eq 4 permits the elimination of two unknown variables from eq 5, α and ϕ_p, for example. Now ΔF^{in} is a function of only two variables, $\Delta F^{in} = f(\phi_W,\phi_B)$, and we can easily find the characteristics of the brush that is in equilibrium with the mixed solvent bulk.

The thermodynamics of the bulk solvent is defined by the chemical potentials of the solvent components in the bulk:

$$\mu_B^{out} = \ln \Phi_B + \chi_{BW}(1-\Phi_B)^2$$
$$\mu_W^{out} = \ln \Phi_W + \chi_{BW}(1-\Phi_W)^2 \tag{9}$$

Here Φ_B and Φ_W are concentrations of the solvent B and water in the bulk solvent connected by the evident relation $\Phi_B + \Phi_W = 1$. Note that the interactions between the solvent B and the ions of water are neglected due to their low concentration, and the

chemical potentials of the ions are defined directly by the entropic contribution. In particular, if Φ_H is the concentration (volume fraction) of protons in the bulk, their chemical potential is

$$\mu_H^{out} = \ln \Phi_H \tag{10}$$

while the chemical potentials of the solvent B and water are independent of Φ_H. Moreover, the main equations written here for the salt-free systems contain no μ_H^{out} term at all. However, the mixing entropy of ions should be taken into account if salt is added.

There are two equivalent ways to find the equilibrium state of the brush.[28] The first one implies that the chemical potentials of the solvent components are equal inside and outside the brush. Another method applied in this paper resides in constructing the excess free energy for the entire system. Two factors, namely, the intrabrush interactions ΔF^{in} and the solvent exchange ΔF^{exch} between the bulk and the brush, should be accounted for:

$$\Delta F^{ex}(\varphi_W,\varphi_B) = \Delta F^{in} + \Delta F^{exch}$$
$$= \Delta F^{in} - \frac{\varphi_B}{\varphi_p}\mu_B^{out} - \frac{\varphi_W}{\varphi_p}\mu_W^{out} \tag{11}$$

The next step is to minimize this quantity with respect to the remaining independent variables and thus to find all equilibrium characteristics of the brush ionized after dipping it into a binary solvent (solvent B/water) with a fixed bulk composition Φ_B. The minimization is carried out numerically, and results from that are discussed in the following section.

2. System with Added Salt. It is well-known that the addition of low molecular weight salt to a polyelectrolyte systems affects them significantly. This is the motivation to consider the corresponding system in the presence of a simple monovalent salt of the NaCl type. We assume the concentration Φ_S in the bulk to be comparatively low. More specifically, it should not exceed the concentration of the ionized polymer segments $\alpha\phi_p$ inside the brush. In this case, the brush is certainly in the osmotic (OsB) regime.[23,25,26] We also assume the salt to be totally dissociated. The negative net polymer charge inside the brush is compensated by the net charge of counterions. However, in the presence of salt, these counterions include not only the intrinsic positive ions H_3O^+ dissociated from the polymer but also Na^+ ions that come from the bulk. More precisely, there is an ionic exchange between the brush and the bulk, which results in an additional ionic contribution to the exchange free energy ΔF^{exch}(ionic). This contribution depends in particular on the chemical potentials μ_I of the ion components in the bulk. If the salt concentration Φ_S in the bulk is well below the water concentration Φ_W at the binodal, the salt presence gives rise to only one additional thermodynamical characteristics of the bulk

$$\mu_{Na} = \ln \Phi_S \tag{12}$$

Equation 9 still stands, and we can consider the ionic contribution to the exchange free energy ΔF^{exch}(ionic). The relative concentrations of the protons and Na^+ ions inside and outside the brush should be equal if no specific interactions exist. Any polymer segment provides the system with α protons, which separate then into two groups: $\alpha\Phi_H/(\Phi_S + \Phi_H)$ is the number of protons remaining inside the brush; $\alpha\Phi_S/(\Phi_S + \Phi_H)$ is the number of protons that leave the brush and mix with the bulk protons of the concentration Φ_H.

On the other hand, there is a fraction of the salt ions that come into the brush to compensate its negative charge: $\alpha\Phi_S/(\Phi_S + \Phi_H)$ is the number of the salt ions coming into the brush (per polymer segment).

This redistribution of the positive charges between the brush and the bulk contributes to the mixing entropy of the entire system. For the salt-free case the term ΔF^{in}(ionic) = α ln $\alpha\phi_p$ in eq 5 gives the mixing entropy of the counterions dissociated from the polymer. If there is a redistribution of mobile protons and ions of the salt, the mixing entropy of counterions involved, into the excess free energy (per polymer segment), is the following:

$$\Delta F^{exc}(\text{ionic}) = \Delta F^{in}(\text{ionic}) + \Delta F^{exch}(\text{ionic}) =$$
$$\alpha\frac{\Phi_H}{\Phi_H+\Phi_S}\ln\frac{\alpha\varphi_p\Phi_H}{\Phi_H+\Phi_S} + \alpha\frac{\Phi_S}{\Phi_H+\Phi_S}\left(\ln\Phi_H + \ln\frac{\alpha\varphi_p\Phi_S}{\Phi_H+\Phi_S} - \ln\Phi_S\right) = \alpha\ln\alpha\varphi_p\frac{\Phi_H}{\Phi_H+\Phi_S} \tag{13}$$

The first term on the second line of eq 13 gives the mixing entropy of the protons remaining in the brush. The remaining three terms concern the mixing entropy of the protons in the bulk, the mixing entropy of Na^+ ions coming into the brush, and the loss in the mixing entropy of these Na^+ ions, which they possessed in the bulk.

After writing the new term responsible for the mixing entropy of positive charges, one should examine the resulting effect on the free energy and a strategy for solving the problem. Fortunately, it is easy to find out that the formalism developed for the salt-free case can be used again with just one complication. After minimization of the free energy with respect to α, one finds that, instead of the effective constant $\tilde{K}^0$ for the reaction of the polymer dissociation given by eq 7, now an effective constant $\tilde{K}$ should be involved:

$$\tilde{K} = \tilde{K}^0\frac{\Phi_S+\Phi_H}{\Phi_H} = K_{eff}\exp(-\varphi_B(2\chi_{Be} - \chi_B - \chi_{BW})) \tag{14}$$

Here $\tilde{K}^0$ is still given by eq 7, while K_{eff} is defined by

$$K_{eff} = K(\Phi_S + \Phi_H)/\Phi_H \tag{15}$$

The $\tilde{K}$ parameter describes the polymer ionization in the brush and is composed of two terms. The first term K_{eff} can be considered as an effective dissociation constant, while the second term accounts for the disadvantage of the ionization in the presence of the nonpolar solvent B. The increase in K_{eff} with increasing salt concentration Φ_S in the bulk corresponds to decreasing acidity inside an annealed polyacid brush that occurs as a result of the Na^+ and H^+ ion exchange. This effect has been discussed in large detail previously.[23]

Substitution of $\tilde{K}$ into the relation for the free energy leads to eq 8, and thus the formalism developed for the salt-free system is valid again. Of course, this does not mean that the pH or the ionic strength does not affect the system significantly. As is clear from eq 14, at $\Phi_S = 0$, the system is salt-free and we have $K_{eff} = K$

irrespective of the Φ_H value. However, the addition of salt, for instance, to a concentration $\Phi_S = 10^{-7}$, will result in a 2 order increase of the value of K_{eff} at $\Phi_H = 10^{-9}$, whereas at $\Phi_H = 10^{-6}$ the effect will be negligible.

C. The Self-Consistent-Field Theory. One can approach the problem more exactly by solving the corresponding self-consistent-field equations. In this paper numerical analysis of SCF equations is carried out in the formalism developed by Scheutjens and Fleer,[22,29] which accounts for an internal inhomogeneous structure of the brush in the direction normal to the grafting surface.

The physics of the system is defined by the solution of the Edwards diffusion equation

$$\frac{\partial G(z,N)}{\partial N} = \frac{1}{6}\frac{\partial^2 G(z,N)}{\partial z^2} - u(z)\, G(z,N) \qquad (16)$$

with the appropriate boundary conditions of an impenetrable wall at $z = 0$ and starting condition $G(z,0) = \delta_z$. Here $G(z)$ is a segment weighting factor, and again z is the direction normal to the surface. Exact analytical solutions for this differential equation are not possible, but accurate numerical methods are available in the limit of lattice approximations.

Most relevant in the present discussion is therefore to specify what contributions are included in the segment potential and how these are computed:

$$u_J(z) = u'(z) + u_J^{FH}(z) + u_J^{elec}(z) + u_J^{pol}(z) \qquad (17)$$

In this equation the subindex on the segment potential refers to the segment types in the system. In the present system, J refers to one of the following eight entities occupying one lattice site: a polymer unit either in a charged state A^- or in the protonated state HA, one of the aqueous components (H_3O^+, H_2O, or OH^-), a molecule of the basic solvent B, or one of the ions Na^+ and Cl^-. In eq 17 four contributions to the segment potential are specified.

The first contribution is a Lagrange field coupled to the incompressibility constraint (eq 3).

The second contribution accounts for short-range nearest-neighbor contact interactions. For ionic species this quantity should include the Born energies.

$$u_J^{FH} = \sum_I \chi_{IJ}(\varphi_I(z-1) + \varphi_I(z) + \varphi_I(z+1) - 3\varphi_I^b)/3 \qquad (18)$$

Here, the Flory−Huggins parameters χ_{IJ} account for the nonelectrostatic pair interactions and are discussed above (here the notation is temporarily generalized to have a simple equation). The summation over I runs again over all segment types, and ϕ_I^b is the concentration of unit I in the bulk (indicated by superindex b). The averaging as done in eq 18 is such that the contact interactions are weighted equally over three consecutive layers. This weighting is performed because it is known to reduce lattice artifacts that manifest themselves at times that there are sharp interfaces in the system. In the present system the solvent B−water interface is actually such a sharp phase boundary.

The third contribution is the usual electrostatic term that is only present for the charged components:

$$u_J^{el} = \frac{\nu_J e\psi(z)}{k_B T} \qquad (19)$$

where ν_J is the valence of unit J. We consider only monovalent ions in this paper, and thus ν only assumes the value 1 or −1 (or 0). As the densities of all components in the system are assumed to be available, we write for the charge density

$$q(z) = \sum_I \nu_I e\varphi_I(z) \qquad (20)$$

This charge density enters in the Poisson equation

$$\frac{\partial\epsilon(z)}{\partial z}\frac{\partial\psi(z)}{\partial z} = -q(z) \qquad (21)$$

For the dielectric permittivity profile a simple density weighted average is implemented:

$$\epsilon(z) = \sum_I \epsilon_{rI}\epsilon_0\varphi_I(z) \qquad (22)$$

Of course, this Ansatz garentees that the dielectric constant is high in the water phase and low in the oil phase. The approximation is expected to be less accurate in the interfacial zone between the water an oil phase. As this interfacial region is very small, i.e., of the size of a water molecule, the error is negligible. Finally, the fourth term, which has been omitted in previous implementations of polyelectrolyte self-consistent-field models, must be introduced. Without this term there is a (minor) thermodynamic inconsistency in the system. In principle, the contribution is present for all the units in the system, irrespective of whether they are charged or not. It accounts for the free energy contribution of bringing a polarizing unit from infinity to a position with electric field $E(z)$. The amount of polarization is proportional to the field, and the energy gain is also proportional to the field. Thus, the combined effect is a term proportional to the field strength squared. In a lattice variant where the dielectric constant varies from layer to layer the result is given by

$$u_J^{pol}(z) = \frac{a\epsilon_0\epsilon_{rJ}}{k_B T}[(\epsilon(z-1) + \epsilon(z))(\psi(z-1) - \psi(z))^2 + (\epsilon(z+1) + \epsilon(z))(\psi(z+1) - \psi(z))^2] \qquad (23)$$

In the model for annealed polyelectrolytes the units in the system are linked by dissociation reactions, eqs 1 and 2, parametrized by the reaction constants K and K_W, respectively. The local degree of dissociation of the various components depends on the interactions felt by the units in various states and the electrostatic potential. The effective pK of for example a polymer unit in the solvent B is not identical to the pK of the same unit in water. This is due to the different Flory−Huggins parameters that can be assigned to the units in the two phases. The self-consistent-field theory applicable for segments with more than one internal state has been discussed in the literature.[30] However, the system under consideration is slightly more complicated, and the approach proposed in ref 30 is modified accordingly. In particular, the water dissociation equilibrium is more accurately accounted for (cf. eqs 1 and 2). Full details will be published elsewhere.

D. Parameters. As is obvious from the above, there are many parameters that should receive proper attention. In principle, we can specify each one of them independently and keep track of how its variation affects the system in general. However, this way is evidently confusing. Hence, for clarity we will make a few simplifying assumptions to manage the set of parameters. Some of these assumptions are already mentioned above, and here they are just included into a general framework.

The first simplification lies in the assumption that all interacting entities in the system, i.e., molecules, ions, or polymer segments, are of the same volume. In the terms of the lattice model, such as the SCF model described above, this means that any unit in the system occupies one lattice site. This is the reason that H_3O^+ ions are considered instead of pointlike protons, and thus, the water ionization is described as a process that develops without an increase in the number molecular entities and, hence, without an increase in the volume. Note that this aspect was not included in the theory of Israels.[30] It is also assumed that the pH value is defined by the concentration of H_3O^+ ions. The Ansatz of equal volumes provides the equivalence between the volume fractions and the relative numbers of molecules for all species. A method of recalculating these characteristics into molar concentrations, as commonly used in experimental investigations, will be discussed further in the final remarks of the paper. For simplification reasons, we assume also that the flexibility of polymer chains is not affected by the type of solvent and is equal both when the solvent is water and when it is oil.

Another simplifying point concerns the Flory−Huggins interaction parameters. We begin with the solvent B. It is assumed that the solvent B repels all charged units (polymer segments A^-, water ions H_3O^+ and OH^-, ions of the salt Na^+ and Cl^-) equally, and these interactions are characterized by the same value of the Flory−Huggins parameter χ_{Be}. Moreover, this parameter is set equal to that of the solvent B with nonionized water. All calculations are carried out for $\chi_{Be} = \chi_{BW} = 3.5$. This strong segregation is used in previous studies as well and is sufficient to generate a sharp oil−water interface in or at the edge of the brush. We further suppose that the solvent B interacts athermal with respect to nonionized polymer units and put $\chi_B = 0$. This means that B is a very poor solvent for the charged units and a good solvent for the noncharged polymer. Actually, this choice mimics hydrophobized polyelectrolyte chains.

In accordence with this, it is assumed that the water component has some repulsive interactions with noncharged polymer segments, i.e., due to their hydrophobic parts, and we set $\chi_W > 0$. In the box model calculations are carried out for a number of the χ_W values within the range $0.2 \leq \chi_W \leq 3.5$. In the SCF calculations we use only one value of this parameter $\chi_W = 0.5$, i.e., water is a Θ-solvent for noncharged polymer. In addition, it is assumed that the same value of χ_W is used for the following water contacts: the nonelectrostatic interactions with small ions and with both the charged and the noncharged polymer segments.

The contribution of electrostatic interactions to the free energy is calculated differently in two models. This difference may be outlined once more. In the box model the charged brush is suggested to hold an equivalent number of mobile counterions and no co-ions. The introduction of a supplementary parameter $K_{eff} = K(\Phi_S + \Phi_H)/\Phi_H$ accounts not only for the dissociation constant of the polymer but also for the ionic composition of the bulk solvent. Once K_{eff} is fixed, the calculations reduce to those for the equilibrium degree of ionization of the polymer. As a result, water appears to be a good solvent for the ionized polymer segments.

In the SCF formalism, the distribution of the small ions in the system is obtained accurately from solving the Poisson−Boltzmann equation. The dielectric constant of water in these calculations is set to 80 and that of the solvent B and polymer to 2, and for the remaining components an intermediate value of 5 was used. Equation 22 calculates the dielectric permittivity of the mixture.

Let us note that, solving the Poisson−Boltzmann equation, one can take into account a part of electrostatic correlation effects, bounded up with the total charge concentration. The specific polymer correlation effects stay out of consideration, and the theory is based on mean-field approximation in this aspect. It is known, however, that these correlation interactions cannot compete with entropy contributions, which dominate in our system.

A few more parameters should be defined for the SCF model. As distinct from the box model wherein the chain length of the grafted polyelectrolyte is not defined, in all SCF calculations we have fixed it to $N = 100$. Each polymer unit contains one dissociable group, so that the maximum number of charges on the chain is also 100. In both models the grafting density, i.e., the number of chains per unit area, was taken to be $\sigma^{-1} = 2/100$, which corresponds to an area-per-molecule of 50 (in units of segment sizes). The substrate onto which the polymers are grafted is assumed, again for simplicity, to be inert; all components, independent of what internal state they are, do not interact specifically with the substrate.

The size of the system, i.e., the number of lattice layers M, was fixed to 200 in all cases. This means that this is twice as large as the maximum extension of the chains. Especially for low ionic strength cases, it is possible that the electrostatic field at the phase boundary did not vanish. The reflecting boundary conditions chosen at $z = M$ then mimicked an opposing brush at a distance of $2M$ of the one we are interested in. We have investigated the effect of the finite size of the system and the conclusion of this is that, to good approximation, the results can be considered as that of an isolated brush.

There are two relevant dissociation constants in the system. For the autodissociation reaction of water we take $pK_W = 17.5$. Taking the conversion of volume fractions to molar concentrations into account (see below), this means that at pH = 7 the proton and hydroxyl concentrations are equal. The second dissociation constant is set to $pK = 6$, which mimics carboxyl groups.

Of course, the present set of parameters is highly idealized. It is expected that a much more detailed parameter analysis is necessary when the theory is used to analyze corresponding experiments.

3. Results and Discussion

A. Box Model. From the above it is clear that we will consider a binary, highly incompatible, solvent mixture and that the main focus will be on phenomena that occur in the pre-binodal concentration region for

the bulk solvent. In this concentration range the mixture is a neat homogeneous one-phase system.

Below we will discuss conformational transitions in the brush. For example, we will refer to a brush immersed in a thin water film as a brush filled by the water phase. However, from the solvents perspective, the system is typically not at bulk coexistence and the water film is necessarily of mesoscopic dimensions. Our nomenclature is convenient to refer to the phase state of the polymer; i.e., it is surrounded by water. We trust that this will not be confusing for the reader.

In the case of the interaction parameter $\chi_{BW} = 3.5$, the binodal value for the added water is $\Phi_W^{bin} \approx 0.037\ 89$. In line with the presented formalism, we use an effective constant K_{eff} defined by eq 15. This parameter provides a simple way of taking all charged units that show up in the system into account. It includes the reaction constant K. The salt concentrations Φ_S and proton concentration Φ_H in the bulk contribute directly.

In the absence of water ($\Phi_W = 0$), there is only one minimum on the free energy "surface". This minimum corresponds to the equilibrium state of the neutral brush in the solvent B. At $\chi_W > \chi_B$, this minimum remains present also with increasing water concentration. At some amount of water in the system another minimum appears. This second minimum corresponds to a partially ionized brush where the polymer chains are surrounded by water. At a particular water concentration $\Phi_W = \Phi_W^{tr}$ the two minima are equal in depth. This corresponds to a transition from a water-poor to a water-rich state of the brush. The value of Φ_W^{tr} is controlled by the values of χ_W and K_{eff}. It should be realized that at given χ_W only the value of $K_{eff} = K(\Phi_S + \Phi_H)/\Phi_H$ controls the ability of the polymer segments to be ionized in the salted water solution.

In Figure 2a a series of thermodynamic characteristics of the brush are presented as a function of the water concentration Φ_W in both pre-binodal $\Phi_W < \Phi_W^{bin} = 0.037\ 89$ and post-binodal $(1 - \Phi_W) < \Phi_W^{bin} = 0.037\ 89$ regions for the bulk. The calculations are carried out for the K_{eff} values 0.01, 0.1, and 0.5. As is seen from Figure 2a, for each value of K_{eff} two branches of the free energy intersect. The point Φ_W^{tr} thus manifests a first-order phase transition, which occurs in the region $\Phi_W^{tr} < \Phi_W^{bin}$. The point of the phase transition shifts toward the binodal as K_{eff} values decrease.

In Figure 2b the degree of the polymer dissociation α is presented. For all values of K_{eff} a transition from essentially a nonionized into an ionized state of the polymer is observed. This occurs with a discrete jump in α from one value to another. It is noteworthy that the magnitude of this jump is almost independent of K_{eff} in the presented range of conditions.

Despite a low value of the water concentration in the pre-binodal region, the brush takes up water due to the tendency of the polymer to dissociate. This effect is clearly demonstrated in Figure 2c where relative concentration ψ_W of water inside the brush is given as a function of the water concentration Φ_W in the bulk. The relative concentration ψ_W of water inside the brush is defined as follows:

$$\psi_W = \frac{\varphi_W + \alpha\varphi_p}{1 - \varphi_p} \tag{24}$$

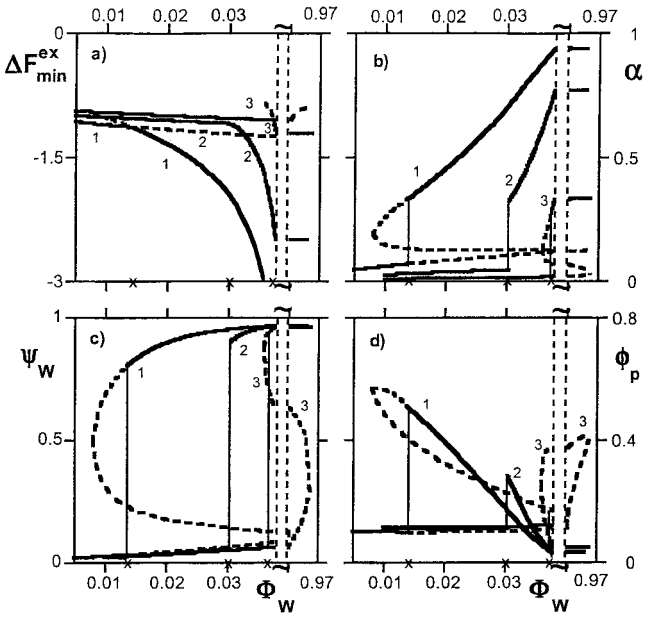

Figure 2. Box model: the thermodynamic characteristics of the brush as functions of the water concentration Φ_W in the bulk. (a) Free energy of the brush ΔF_{min}^{ex}. (b) Degree of ionization of polymer segments α. (c) Relative water fraction ψ_W. (d) Polymer density ϕ_p. The solid curves 1−3 represent stable states of the brush; the dashed curves 1−3 are metastable and unstable states. The x-sign on the x-axis gives the positions of Φ_W^{tr}. The pre-binodal ($\Phi_W < \Phi_W^{bin} = 0.037\ 89$) and the post-binodal ($\Phi_W > 1 - \Phi_W^{bin}$) regions of the bulk are divided with the $\sim$ sign on the Φ_W axis. The dashed verticals mimic the two-phase state of the bulk. The parameters are $K_{eff} = 0.5$ (curves 1), 0.1 (curves 2), and 0.01 (curves 3); $\sigma = 50$, $\chi_{BW} = \chi_{Be} = 3.5$, $\chi_B = 0$, and $\chi_W = 0.5$.

The brush absorbs water at any considered value of K_{eff}. The first-order phase transition from a water-poor brush to a water-rich one occurs again as a jump in the relative concentration of water ψ_W inside the brush from near zero up to a value only slightly less than unity.

The change in the polymer density ϕ_p is of profound interest. In Figure 2d ϕ_p is presented as a function of the water concentration Φ_W in the bulk. At the point of the phase transition a jump in the polymer density is evident. However, the magnitude of the jump depends significantly on K_{eff}. At $K_{eff} = 0.5$, the phase transition ($\Phi_W^{tr} \approx 0.015$) occurs relatively far from the binodal and is accompanied by a pronounced polymer collapse: the polymer density changes from $\phi_{p1} \approx 0.1$ in the water-poor phase up to $\phi_{p2} \approx 0.5$ in the water-rich phase. With the following addition of water to the bulk solvent, a relaxation is observed, and the polymer density decreases smoothly up to the value $\phi_p \approx 0.025$ at the binodal. At $K_{eff} = 0.1$, the point of the phase transition ($\Phi_W^{tr} \approx 0.03$) is much closer to the binodal, and the polymer collapse is not as pronounced as at $K_{eff} = 0.5$: the polymer density in the water poor phase is almost the same, $\phi_{p1} \approx 0.1$, while at the transition it reaches only the value $\phi_{p2} \approx 0.3$. Finally, at $K_{eff} = 0.01$, the point of the phase transition ($\Phi_W^{tr} \approx 0.036$) is very close to the binodal value, and the polymer behavior under the phase transition differs qualitatively from that at $K_{eff} = 0.5$ and 0.1. Instead of a collapse, there is a jumplike transition toward a more relaxed state with $\phi_{p2} \approx 0.07$.

In Figure 3 the same characteristics are shown for a highly hydrophobic ($\chi_W = 3.5$) ionizable brush. In this case the values of K_{eff} should be increased before the

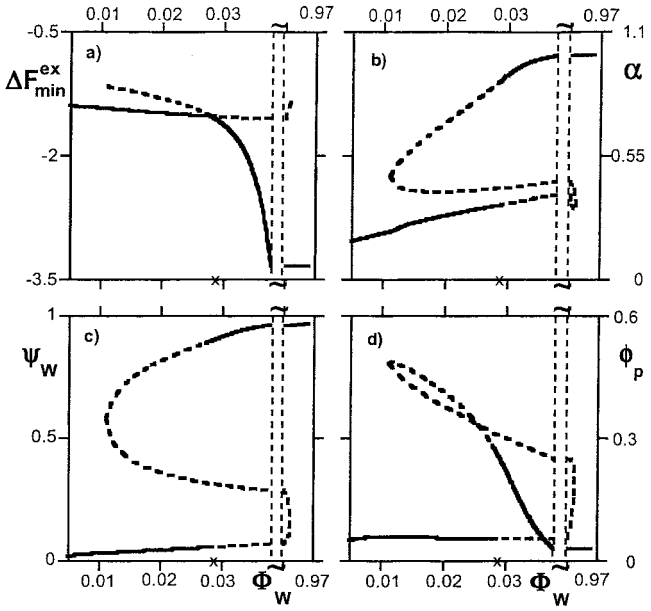

Figure 3. Box model: the thermodynamic characteristics of the brush as functions of the water concentration Φ_W in the bulk similar to Figure 2. (a) Free energy of the brush ΔF^{ex}_{min}. (b) Degree of ionization of polymer segments α. (c) Relative water fraction ψ_W. (d) Polymer density ϕ_p. Parameters: $K_{eff} = 5$ and $\chi_W = 3.5$. Other parameters and characteristics similar to Figure 2.

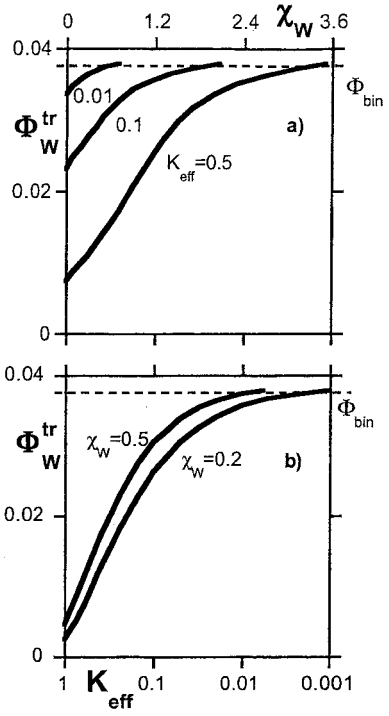

Figure 4. Box model: the position of the phase transition Φ^{tr}_W as a function of (a) the water−polymer interaction parameter χ_W where the K_{eff} values are indicated at the curves. (b) The effective ionization constant K_{eff} where χ_W values are marked at the curves. (The logarithmic K_{eff} axes are reversed.) Other parameters are as in Figure 2.

phase transition can be observed. In Figure 3 an example is shown for $K_{eff} = 5$.

The points of the phase transition Φ^{tr}_W are presented in Figure 4 as functions of χ_W at fixed values of K_{eff} (Figure 4a) and of K_{eff} for fixed values of χ_W (Figure 4b). Other characteristics of the brush in the water-poor and

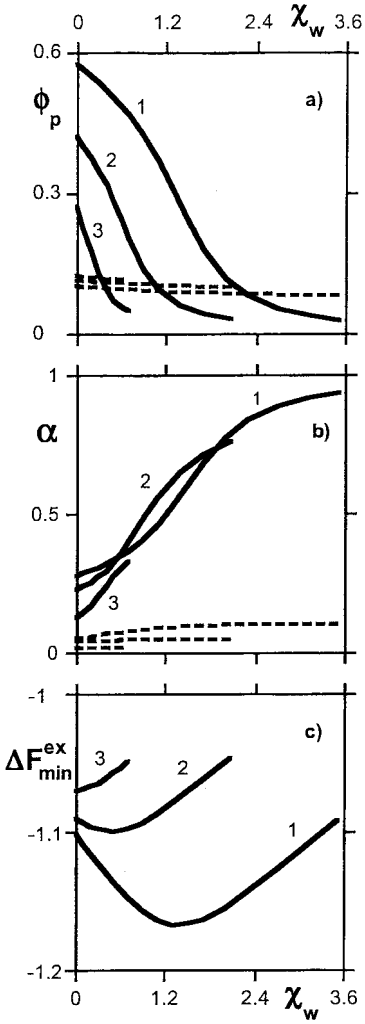

Figure 5. Box model: characteristics of the brush in coexisting water-rich phase (solid curves) and water-poor phase (dashed curves) at the point of the phase transition. Dependencies on χ_W: (a) Polymer density ϕ_p. (b) Degree of ionization α. (c) Free energy of the brush ΔF^{ex}_{min}. $K_{eff} = 0.5$ (curves 1), 0.1 (curves 2), and 0.01 (curves 3). Other parameters are as in Figure 2.

water-rich phases at the point of the phase transition are presented in Figure 5a−c and 6a,b. The corresponding data for the relative concentration of water ψ_W inside the brush are not included since this parameter is very close to unity in all cases, except for extremely low values of $\Phi^{tr}_W < 0.01$ where it drops to $\psi_W \approx 0.8-0.9$.

The authors already discussed in refs 12 and 13 the spectacular exchange of solvents that may occur in the neutral brush: one component of the incompatible mixture is swapped with the other. In the box model this can occur either continuously or as a phase transition depending on the system parameters.[12] As is seen from Figures 2−6, for ionizable brushes the solvent exchange always occurs as the first-order phase transition with jumps both in α and in ψ_W. The change of the polymer density ϕ_p at the transition deserves a more detailed discussion. In the case of a nonionizable brush the change from a good solvent to a better one is necessarily accompanied by a, indeed anomalous, collapse of the brush. However, in the case of an ionizable brush, the transition pattern is even more anomalous: the brush collapse occurs despite its ionization! The extent of the brush collapse is evidently dictated by the

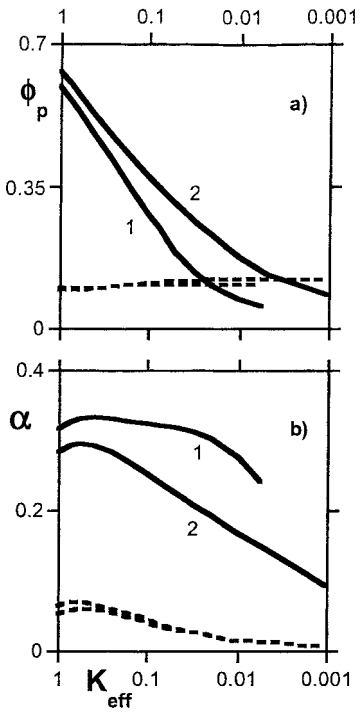

Figure 6. Box model: characteristics of the brush in coexisting water-rich phase (solid curves) and water-poor phase (dashed curves) at the point of the phase transition. Dependencies on K_{eff}: (a) Polymer density ϕ_p. (b) Degree of ionization α. $\chi_W = 0.5$ (curves 1) and 0.2 (curves 2). The logarithmic K_{eff} axes are reversed. Other parameters are as in Figure 2.

spacing between Φ_W^{tr} and Φ_W^{bin}. As is seen from Figures 5a and 6a, the polymer density ϕ_p in the water-rich phase decreases with increase in χ_W at fixed values of K_{eff} or with a decrease in K_{eff} at fixed values of χ_W; after reaching the value of ϕ_p in water-poor phase, it continues to decrease. As a result, the anomalous collapse can even be replaced by a (ordinary) swelling at the transition point. Consequently, at any χ_W, one can find such a value of K_{eff} that ϕ_p does not change at the transition point. However, the transition is still of first order since α and ψ_W change discretely, and even the $\phi_p - \Phi_W$ dependence is not smooth. This difference demonstrates a bend instead of a jump.

All functions presented in Figures 4−6 are monotonic with χ_W and K_{eff} except for the free energy $\Delta F^{ex}(\chi_W)$ of the brush at the transition point as shown in Figure 5c. Comparing parts c and b of Figure 5, one can conclude that a decrease in ΔF^{ex} in the region preceding its minimum is related to a more than linear increase in ionization observed in the same region. Meanwhile, the increase in ΔF^{ex} after passing the minimum occurs due to the increase in χ_W.

Let us pay attention to the conditions needed for the phase transition in the range of low water concentration Φ_W in the bulk. The calculations show that when the polymer is only slightly hydrophobic ($\chi_W = 0.5$), the water can only be competitive with the athermal solvent B ($\chi_W = 0$) for high values of K_{eff}. It is noticeable that these values of K_{eff} exceed the typical values for the dissociation constants K of a weak polyacid by several orders of magnitude. Thus, the ratio Φ_S/Φ_H, i.e., concentrations of the ions Na^+ and H^+ (or H_3O^+), should be large to get high enough value of K_{eff}. To put it another way, at $\Phi_W \ll \Phi_W^{bin}$, only a high enough concentration of salt in the water can make the polyelectrolyte brush to prefer water over the solvent B. It should be noted that we consider only the OsB regime, and this imposes an upper limit to the salt concentration.

So far, only equilibrium states of the brush in the box model were discussed. However, the data presented in Figures 2 and 3 are much richer since metastable and unstable states are also depicted. Interestingly, for the degree of the polymer dissociation α (Figures 2b and 3b) and the relative concentration ψ_W of water inside the brush (Figures 2c and 3c) given as functions of Φ_W, the usual van der Waals loops are obtained, whereas for the polymer density ϕ_p vs Φ_W (Figures 2d and 3d) at the anomalous collapse, the loops in the true sense of the word appear. For a nonionizable brush the loops of this kind were also obtained, and their nature was discussed in ref 28.

Another point of interest is the position of the loop. In Figures 2 and 3 two regions of the bulk composition outside the binodal are presented, i.e., at low concentration of water $\Phi_W < \Phi_W^{bin}$ and at prevailing concentration of water $\Phi_W > 1 - \Phi_W^{bin}$. All phase transitions in Figures 2 and 3 occur in the first region, but there exists values of K_{eff}, for which the van der Waals loops passes the biphasic region (where the values of the chemical potentials in the equilibrium bulk are fixed) and ends in the post-binodal region after crossing the binodal. This means that for the chosen set of the parameters the metastable water-poor phase of the brush exists even in the water-rich phase of the bulk, though for the equilibrium phase this is not the case.

B. The Self-Consistent-Field Calculations. The SCF model allows the investigation of both the thermodynamic characteristics of the entire brush, as well as many details of its internal structure. The last aspect is definitely an advantage of the SCF model, but let us first focus on the overall brush characteristics. This will allow us to compare the SCF results with those obtained for the box model (section 3A). This is an appropriate way to investigate the validity of the box model which is of course relatively efficient in predicting general features for the systems of this type.

1. The Effect of Salt. In Figure 7 the following results of the SCF calculations are presented as a function of the concentration $\Phi_W < \Phi_W^{bin}$ of the water added to the basic solvent B in the bulk: the free energy (Figure 7a), the averaged degree of the polymer dissociation α (Figure 7b), and the averaged polymer density ϕ_p (Figure 7c).

At the salt concentration $\Phi_S = 10^{-5}$, a first-order phase transition occurs at $\Phi_W^{tr} = 0.025$ (Figure 7). The following observations support this: two distinct branches in the free energy cross at the point Φ_W^{tr}. At the same point jumps in the average values of α and ψ_W are observed, and indeed the collapse of the brush is evident. At $\Phi_S = 10^{-6}$, the point of the phase transition Φ_W^{tr} is shifted toward the bimodal, while at $\Phi_S = 10^{-4}$, the considered range $0.01 < \Phi_W < \Phi_W^{bin}$ of the water concentration in the bulk is actually in the post-transition region.

This sequence occurs in the same manner as for the box model as presented in Figure 2, where the dependence of K_{eff} is shown. However, an ionic composition of the bulk solvent is specified somewhat differently in the two models, and the results of the calculations cannot be compared immediately.

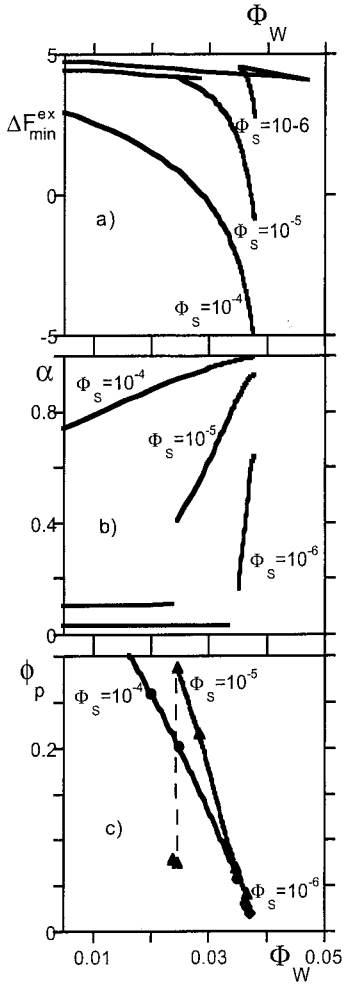

Figure 7. SCF calculations: (a) Free energy of the brush (top). (b) Degree of ionization of the polymer segments α (middle). (c) Polymer density ϕ_p, as functions of the water concentration Φ_W in the bulk (bottom). Chain length $N = 100$; degree of the water dissociation $\alpha_W = 10^{-9}$; the values of the salt concentration Φ_S are indicated. Other parameters are as in Figure 2.

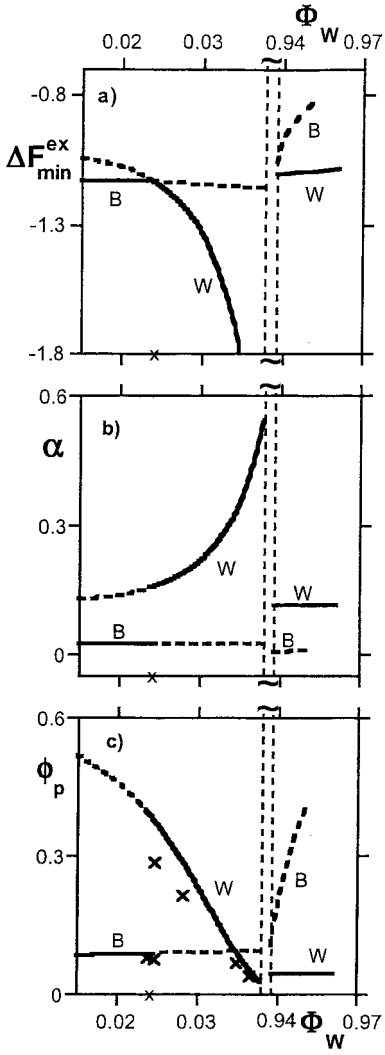

Figure 8. Box model: calculations at $\Phi_S = 10^{-5}$ and $\eta = 0.55$. (a) Free energy of the brush ΔF^{ex}_{min}. (b) Degree of ionization of polymer segments α. (c) Polymer density ϕ_p. Crosses in (c) represent averaged SCF data (see Figure 7). The labels B and W refer to the main solvent that is present in the brush for the indicated conditions. Other designations and parameters are similar to Figure 2.

2. Approximation by K_{eff} and Comparison with the Box Model. In the box model K_{eff} is the only parameter, and every series of calculations is carried out at a fixed value of K_{eff}. Both concentrations Φ_S and Φ_H of Na^+ ions and protons in the box model depend on the water content in the system, but their ratio Φ_S/Φ_H is assumed to be fixed irrespective of the bulk composition. Since the water acidity is also fixed, this means that salted water is added to the basic solvent.

However, the concentrations of Na^+ ions and protons (or H_3O^+) are specified differently in the SCF calculations. Protons appear in the bulk as a result of the dissociation of water, and the degree of the dissociation of water α_W is chosen as a parameter. Setting $\alpha_W = 10^{-9}$, we keep neutral conditions in the bulk (see below for details). Accordingly, the relation $\Phi_H = \alpha_W\Phi_W$ defines the concentration of protons (or H_3O^+) in the bulk. An average concentration Φ_S of Na^+ ions is prescribed regardless of the water concentration Φ_W in the bulk or, in other words, salt is added to the mixed solvent.

We now commence with a detailed comparison of the SCF results with those obtained for the box model. It is necessary to emphasize that in the context of the box model the effective dissociation constant K_{eff} is the only parameter. This parameter depends on the salt concentration in the system. More exactly, K_{eff} is defined by the ratio Φ_S/Φ_H (eq 15). According to the scheme of the SCF calculations, the ratio Φ_S/Φ_H is a function of the bulk composition Φ_W, i.e., $\Phi_S/\Phi_H = \Phi_S/\alpha_W\Phi_W \sim \Phi_W^{-1}$, and therefore K_{eff} is also a function of the bulk composition:

$$K_{eff} = K\frac{\Phi_S}{\alpha_W}\frac{1}{\Phi_W} \qquad (25)$$

The parameters for the SCF calculations are chosen by setting the dissociation constant of the polymer units $K = 10^{-6}$ and the degree of the water dissociation $\alpha_W = 10^{-9}$ (section 2D). Hence, an estimation for K_{eff} in the pre-binodal region is $K_{eff} \le 10^3\Phi_S/\Phi_W^{bin} \approx 2.5 \times 10^{-4}\Phi_S$. In line with this, at $\Phi_S = 10^{-4}$, 10^{-5}, and 10^{-6} we have $K_{eff} > 2.5$, 0.25, and 0.025, respectively. This also indicates that our choice of the K_{eff} values for the box model investigating was very reasonable.

In Figures 8 and 9 ΔF^{ex}, α, and ϕ_p calculated in the box model are shown as functions of the water concentration Φ_W in the bulk. The pre-binodal $\Phi_W < \Phi_W^{bin}$ and

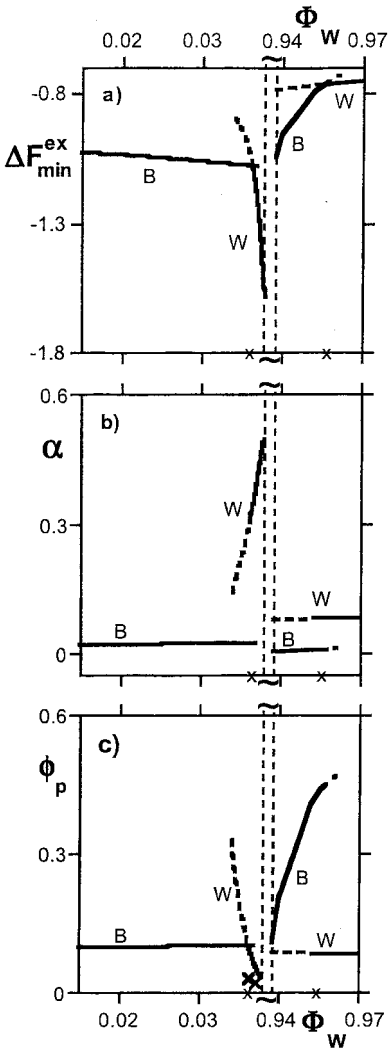

Figure 9. Box model: calculations at $\Phi_S = 10^{-6}$ and $\eta = 0.75$. (a) Free energy of the brush ΔF^{ex}_{min}. (b) Degree of ionization of polymer segments α. (c) Polymer density ϕ_p. The view graphs *a*−*b*−*c* shows the pre-binodal and the post-binodal regions of the bulk, and *a*′−*b*′−*c*′ represents the whole range of Φ_W. Other parameters and characteristics are as in Figure 8.

the post-binodal $\Phi_W > 1 - \Phi_W^{bin}$ regions of the bulk as well as the biphasic region (Figure 9a′−c′ are presented. The box calculations are carried out at $\Phi_S = 10^{-5}$ (Figure 8) and $\Phi_S = 10^{-6}$ (Figure 9); the K_{eff} value is set to $K_{eff} = \eta K(\Phi_S + \alpha_W\Phi_W)/\alpha_W\Phi_W$ (eq 25), where the adjustable parameter η is introduced to give a good fit of the points in the both models, namely, $\eta = 0.55$ at $\Phi_S = 10^{-5}$ and $\eta = 0.75$ at $\Phi_S = 10^{-6}$. As is obvious from Figures 8c and 9c, the SCF results in the region $\Phi_W < \Phi_W^{bin}$ are well described by the box model with K_{eff} depending on the relation between concentrations of protons and Na^+ ions. The box model with K_{eff} decreasing as the water concentration Φ_W in the bulk decreases also demonstrates a possibility to observe fascinating effects in both the post-binodal and biphasic regions of the bulk. First we consider the system at $\Phi_S = 10^{-5}$. In the post-binodal water-rich phase of the bulk the increase in the proton concentration Φ_H and the resulting fall in K_{eff} leads to an increase in the free energy of the brush (Figure 8a) and to a decrease in the degree of the polymer dissociation α (Figure 8b). The brush characteristics are obviously affected by the phase content within the biphasic region of the bulk and are not the same at the two branches of the binodal.

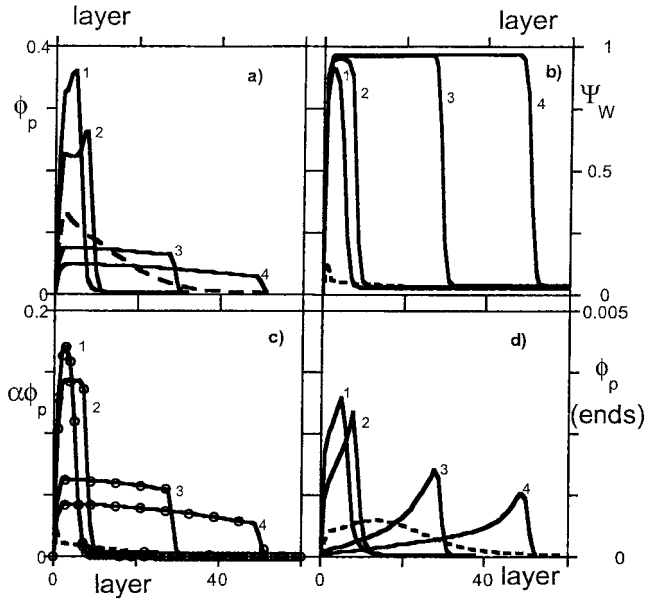

Figure 10. SCF calculations: Density profiles of (a) polymer segments, (b) relative concentration of water, (c) charged polymer segments (lines) and the density of the Na^+ ions (symbols), and (d) free end segments of the grafted chains. Pretransition profiles ($\Phi_W = 0.0237$) are shown by dotted lines. The numbers 1−4 refer to $\Phi_W = 0.0245$, 0.0282, 0.0348, and 0.0365, respectively. Salt concentration $\Phi_S = 10^{-5}$; all other parameters are as in Figure 2.

This effect appears to be even more pronounced at $\Phi_S = 10^{-6}$ (Figure 9), i.e., with decreasing concentration of the salt Φ_S in the bulk. In this case the value of K_{eff} in the post-binodal region $\Phi_W > 1 - \Phi_W^{bin}$ is too low to initiate ionization of the brush, $\alpha \approx 0.03$. Therefore, the solvent B in this region appears to be better for the brush than water. Addition of the B solvent to the bulk water in the post-binodal state of the bulk should induce a transition in the brush into the water-poor phase. This transition is an analogue of that described previously for a noncharged brush.[12−14] An anomalous collapse of the brush occurs at the point of the phase transition, followed subsequently by a relaxation of the brush when the minor solvent (the solvent B in this case) is added. This means that the brush states at the two branches of the binodal are different, and as is shown in Figure 9a′−c′, one more phase transition should occur in the biphasic region of the bulk. Hence, for the system under consideration the theory predicts a possibility to observe three phase transitions inside the brush just varying the phase state of the bulk solvent. With increase in Φ_W, the following sequence occurs: from the water-poor to the water-rich phase of the brush in the pre-binodal region of the bulk, reentry to the water-poor phase in the biphasic region, and again from the water-poor to the water-rich phase in the post-binodal region. The reentry phase transition from water-rich to water-poor phase that happens in the biphasic domain of the bulk is apparently anomalous because the water contents inside and outside the brush change in opposite directions. The overall process can be specified as a successive forward−reentry−forward phase transition.

3. Detailed Structure of the Brush. The numerical SCF theory gives access to (numerically exact) SCF results of the polyelectrolyte brush in the mixed solvent. In particular, there is a wealth of information on the spatial distributions of various quantities in the brush. A selection of such profiles is presented in Figure 10.

The polymer density profile ϕ_p is given in Figure 10a. The profile of the relative concentration ψ_W of water inside the brush may be found in Figure 10b. The distributions of charged polymer units $\alpha\phi_p$ as well as that of Na^+ ions inside the brush are collected in Figure 10c. Finally, the distribution of the chain ends may be found in Figure 10d. The data are obtained for a series of the water concentrations Φ_W at the fixed value of the salt concentration $\Phi_S = 10^{-5}$ in the bulk, corresponding to the most pronounced phase transition in Figure 7 that occurs at $\Phi_W^{tr} \approx 0.0245$.

The dotted curves show the water-poor phase existing at the lower values of $\Phi_W < \Phi_W^{tr}$ (in particular, $\Phi_W = 0.0237$ in Figure 10). In the water-poor phase all characteristics are typical for the neutral brush in a single solvent. Indeed, the solvent is essentially pure since the relative concentration ψ_W of water inside the brush is negligible (Figure 10b), and therefore the ionization of the polymer is absent (Figure 10c). As a result, the polymer density profile ϕ_p is more or less parabolic (Figure 10a), and the chain ends are distributed smoothly (Figure 10d).

Curves 1 in Figure 10 show the structure of the brush in the water-rich phase at the point of the phase transition ($\Phi_W^{tr} \approx 0.0245$). The brush is just filled by water (Figure 10b); the polymer collapsed and just reached its maximum density of $\phi_p \approx 0.35$ (Figure 10a). The density of the charged polymer units is also very high, $\alpha\phi_p \approx 0.17$ (Figure 10c). The brush is collapsed into a rather slender compact structure (it occupies no more than 10 lattice layers) of almost uniform density, and thus the distribution of the chain ends also differs strongly from that in the water-poor phase (Figure 9d). The most remarkable point is that the end-point distribution has a pronounced maximum at the outer border of the brush.

Curves 2−4 in Figure 10 demonstrate the successive relaxation of the brush as the water concentration Φ_W in the bulk increases. The brush is always fully hydrated (Figure 10b), and the polymer, being in the water-rich phase, is highly ionized (Figure 10c). However, the brush is still very far from the structure typical of that in pure water: the polymer density profiles ϕ_p (Figure 10a) show that the brush is collapsed, but not as much as at the point of the phase transition (curve 1). The end-point distributions still feature a peculiar sharp maxima at the outer border of the brush. Inspection of these profiles in Figure 10 gives clear insight into why this system is so well described by the box model. Most of the assumptions put in the box model are accurately realized in the full calculations. For example, in all the cases it is true that the concentration of Na^+ ions inside the brush (shown by circles in Figure 10c) follows the corresponding profile of the charged polymer density $\alpha\phi_p$. Hence, the net polymer charge is compensated exactly by the net charge of Na^+ ions drawn in from the bulk and the assumption of local electroneutrality of the system is fulfilled. Also, the end points are predominantly on the edge of the brush, and the overall profile resembles a steplike function.

4. The Brush at the Boundary between the Solvent Components. As is seen from Figure 10, the end-point distributions of the polymer chains show nontrivial singularities at the border of the brush. The result is not surprising because a sharp border between the water and the solvent B is evidently energetically unfavorable. The polymer segments tend to adsorb their uncharged units onto this interface. This is illustrated in the final figure. In Figure 11 both the densities of dissociated and nondissociated polymer units are given as functions of distance from the surface. The relative concentrations of water and solvent B are also presented. It is interesting to note how the density of nondissociated polymer units coincides exactly with the border between water and solvent B. The inability to charge the polymer units at the interface may in part be due to the relatively low dielectric permittivity of the B-phase. At the boundary the dielectric permittivity is already dropping. Putting many charges near this boundary would cause the electrostatic potential to be locally high, which then needs to decay in the B-phase.

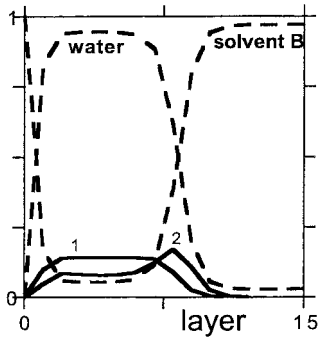

Figure 11. SCF calculations: Density profiles of dissociated (1) and nondissociated polymer segments (2), water and solvent B. $\Phi_W = 0.0282$, $\Phi_S = 10^{-5}$; all other parameters are as in Figure 2.

5. Experimental Aspects. Most of the variables in the system are expressed in dimensionless units. However, molar concentrations are typically used in experiments and parameters such as the pH value, the ionization constants for polyacid and water, and the salt content are typically defined in mol/L. To have an opportunity of comparing model investigations with those carried out for realistic systems, we need a way to recalculate the data. We can suggest the following steps to make the translation. Let us take the molecular mass of water $M = 18$ as a starting point. Then 1 L contains 55 mol of water, and we find easily a linkage between dimensionless (theory) and molar (real) characteristics of the system:

$$\frac{\Phi_H(\text{theory})}{C_H(\text{real})} = \frac{K_W(\text{theory})}{K_W(\text{real})} = \frac{K(\text{theory})}{K(\text{real})} = \frac{\Phi_S(\text{theory})}{C_S(\text{real})} \approx 0.02 \quad (26)$$

Here C_S is the molar salt concentration, and the last proportionality is written with the assumption that Na^+ and H_3O^+ are identical ions having identical molecular masses. The SCF calculations in this paper are carried out at $\Phi_H = 10^{-9}$, and according to eq 26, this value corresponds to pH ≈ 7, i.e., to neutral conditions in the system.

It should be mentioned that there are possibilities to prepare polyelectrolyte brushes in a controlled way.[31,32] Here the grafting density and the chain length of the brush can (in principle) be accurately tuned. The pH titration of such polyelectrolyte brushes has been performed and followed by optical reflectometry.[31] Thus, the technology to investigate the behavior of the solvents and polyelectrolytes in the weak polyelectrolyte brush is available.

4. Summary and Conclusions

We have used the Alexander−de Gennes box model and a numerical SCF method to study the problem of end-grafted annealed polyelectrolyte chains in a mixture of nonpolar solvent with water. We consider amphiphilic weak polyelectrolytes that are soluble in both water and organic solvent B. Hydrophobic groups cause solubility in the solvent B while in water it occurs due to ionization. It is assumed that the solvent exists as a one-phase mixture only in rather narrow pre-binodal (very low content of water) and post-binodal (prevailing content of water) regions. Many interesting phenomena are reported for this system.

It is shown that water can expel oil (solvent B) from the brush even if the brush is immersed into a mixture of a very low water concentration (pre-binodal composition of the bulk). Furthermore, if salt is added, it appears as the third solvent component and affects the system significantly, being an additional source of counterions with respect to the ionized polymer segments. This paper deals with a polyacid brush and a monovalent salt (NaCl, for example) that is totally ionized in the solvent. We conclude that the solvent replacement inside the brush occurs if Na^+ concentration in the bulk exceeds H^+ concentration by a few orders. Salted water (salt concentration is very low, $10^{-2}-10^{-3}$ mol/L) competes with oil in the pre-binodal region and can be taken up by the brush. However, under the same conditions pure water (with no salt added) appears to be uncompetitive with oil.

It is also shown that different scenarios are possible for the solvent exchange inside the brush, which occur as a phase transition with increasing water concentration Φ_W in the bulk. Adding water with a given salt concentration to the major solvent, one can observe a solvent exchange inside the brush and a transition into the water-rich phase. This occurs either in the pre-binodal (at high enough concentration of the salt in water) or in the post-binodal regions of the water concentration Φ_W in the bulk. If the bulk is segregated into two phases, the brush state is independent of the overall concentrations of the solvent components.

The whole picture appears to be more complicated if the salt concentration is fixed in the bulk regardless of the water concentration Φ_W. The calculations show a possibility of three successive phase transitions in the brush as the water concentration Φ_W in the bulk increases: two transitions into the water-rich phase, one of them being in the pre-binodal region, while another one occurs in the post-binodal region of the bulk, and another (reentry) transition, which can be observed in the biphasic region of the bulk.

Very characteristically we find, similarly as discussed for neutral brushes, that the polymer chains can collapse into the good solvent. Indeed, if the point of the phase transition into the water-rich phase Φ_W^{tr} is significantly lower than the bulk binodal value Φ_W^{bin}, the phase transition is accompanied by an abnormal collapse of the brush. This effect decreases as the value of Φ_W^{tr} approaches the binodal value Φ_W^{bin} and can be even of the opposite sign; i.e., under the phase transition, the brush stretching can be observed.

The formation of the water-rich state in the brush relates directly to its ionization and occurs as a first-order phase transition. However, it is worth noting that this phase transition is rather special. Indeed, according to the results of a number of investigations, it is typical just for the box model that the new phase occurs as a jump involving the whole brush, while the SCF theory gives a much more detailed picture.[11−13,14,28,33] This theory shows that there is typically a wide range of parameters for which two-phase coexistence is observed. In this paper the SCF calculations are performed for comparatively short chains ($N = 100$), and this does not permit microphase segregation to be found.

Let us note that the results obtained in this paper are based on the application of laterally homogeneous models. Direct simulations of the collapse of polymer layers in bad solvent and more elaborate theoretical models show that, depending on grafting density and chain length proportions, there might exist both a laterally homogeneous structure and a heterogeneous "biphase" structure. This state could be represented as a two-dimensional lattice, containing more or less collinear micelles, grafted to the surface with there stretched parts (see, for example, ref 34). More complicated SCF modeling proved that the characteristics of phases and the conditions at which a new phase appears are well predicted even with the naive box model. Thus, there is good reason to believe that the general conclusions of the present theory can be applied to real systems. However, the issue of the initial geometry of the water-rich film, i.e., going beyond the lateral homogeneity assumption used in the present analysis, remains to be solved.

Another interesting feature of the system is related to the degree of charging of polymer segments that adsorb on the oil−water interface. At the transition and in the post-transition region the brush engulfs itself in water. This effect gives rise to a sharp boundary between incompatible solvent components at the periphery of the brush. This phase boundary appears to be an additional attractor for the polymers, and as a result, the SCF calculations show an increase in the polymer concentration there. Moreover, in the considered system any polymer segment can be ionized independently of its position along the chain, and thus it is nonionized polymer segments that significantly enrich the boundary.

The main part of this investigation is carried out in the formalism of the box model. Good agreement of the results with those of the SCF calculations verifies the additional electrophysical approximations that are on the basis of the box model for this particular system: (i) the local electroneutrality of the system and (ii) the introduction of an effective constant of the polymer ionization as a function of the ionic composition of the solvent. As a result, we conclude that the box model does again an excellent job in predicting general features of the behavior of a polyelectrolyte brush. The agreement between two models is not only qualitative, but in many aspects even semiquantitative. Certainly, the SCF calculations give much more detailed information about the brush structure than that obtained using the box model. However, these detailed results show that in this particular system the brush can be perfectly described by the most simple box model. The success is attributed to its stepwise structure.

Let us emphasize finally that the effects discussed in this paper are quite general, and from this point of view, the polymer brush can be considered as a convenient model to investigate properties of more complicated polymer systems in mixed solvents.

Acknowledgment. This work was partially supported by NWO Dutch-Russian programs "Polyelectrolytes in Complex Fluids" and "Self-organization and Structure of Bio-nanocomposites" by RFBR (Grant 99-03-33319) and the Russian Federal Program "Integration" . J.v.M acknowledges support for CW-NWO.

References and Notes

(1) de Gennes, P. *Macromolecules* **1980**, *13*, 1069.
(2) Milner, S. T. *Science* **1991**, *251*, 905.
(3) Halperin, A.; Tirrel, M.; Lodge, T. *Adv. Polym. Sci.* **1992**, *100*, 31.
(4) Birshtein, T.; Amoskov, V. *Polym. Sci.* **2000**, *C42*, 172.
(5) Leermakers, F.; Zhulina, E.; van Male, J.; Mercurieva, A.; Fleer, G. J. Birshtein, T. *Langmuir* **2001**, *17*, 4459.
(6) Lai, P.-Y.; Halperin, A. *Macromolecules* **1992**, *25*, 4134.
(7) Marko, J. *Macromolecules* **1993**, *26*, 313.
(8) Marko, J.; Johner, A.; Marques, C. *J. Chem. Phys.* **1993**, *99*, 10.
(9) Johner, A.; Marques, C. *Phys. Rev. Lett.* **1992**, *69*, 1827.
(10) Birshtein, T.; Lyatskaya, Y. *Macromolecules* **1994**, *27*, 1256.
(11) Lyatskaya, Y.; Balazs, A. *Macromolecules* **1997**, *30*, 7588.
(12) Birshtein, T.; Zhulina, E.; Mercurieva, A. *Macromol. Theory Simul.* **2000**, *9*, 47.
(13) Mercurieva, A.; Leermakers, F.; Birshtein, T.; Fleer, G.; Zhulina, E. *Macromolecules* **2000**, *33*, 1072.
(14) Leermakers, F.; Mercurieva, A.; Birshtein, T.; Zhulina, E.; van Male, J.; Besseling, N. *Langmuir* **2000**, *16*, 7082.
(15) Alexander, S. *J. Phys. (Paris)* **1977**, *38*, 977.
(16) Semenov, A. *Zh. Eksp. Teor. Fiz.* **1985**, *84*, 733.
(17) Skvortsov, A.; Gorbunov, A.; Pavlushkov, I.; Zhulina, E.; Borisov, O.; Pryamitsyn, V. *J. Polym. Sci.* **1988**, *30*, 1706.
(18) Zhulina, E.; Pryamitsyn, V.; Borisov, O. *Vysokomol. Soed.* **1989**, *A31*, 185.
(19) Milner, S.; Witten, T.; Cates, M. *Europhys. Lett.* **1988**, *5*, 413.
(20) Milner, S.; Witten, T.; Cates, M. *Macromolecules* **1988**, *21*, 2610.
(21) Zhulina, E.; Borisov, O.; Pryamitsyn, V.; Birshtein, T. *Macromolecules* **1991**, *24*, 140.
(22) Fleer, G.; Cohen-Stuart, M.; Scheutjens, J.; Cosgrove, T. In *Polymer at Interfaces;* Chapman and Hall: London, 1993.
(23) Zhulina, E.; Birshtein, T.; Borisov, O. *Macromolecules* **1995**, *28*, 1491. 24. Lyatskaya, Y.; Leermakers, F.; Fleer, G.; Zhulina, E.; Birshtein, T. *Macromolecules* **1995**, *28*, 3562.
(24) Pincus, P. *Macromolecules* **1991**, *24*, 2912.
(25) Borisov, O.; Birshtein, T.; Zhulina, E. *Macromolecules* **1994**, *27*, 4795.
(26) Pryamitsyn, V.; Leermakers, F.; Fleer, G.; Zhulina, E. *Macromolecules* **1996**, *29*, 8260.
(27) Birshtein, T.; Zhulina, E.; Mercurieva, A. *Macromol. Theory Simul.* **2001**, *10*, 719.
(28) Scheutjens, J.; Fleer, G. *J. Phys. Chem.* **1979**, *83*, 1619.
(29) Israels, R.; Leermakers, F.; Fleer, G. *Macromolecules* **1994**, *27*, 3087.
(30) Currie, E.; Sieval, A.; Fleer, G.; Cohen Stuart, M. *Langmuir* **2000**, *16*, 8324.
(31) Mir, Y.; Auroy, P.; Auvray, L. *Phys. Rev. Lett.* **1995**, *75*, 2863.
(32) Klushin, L.; Birshtein, T.; Amoskov, V. *Macromolecules* **2001**, *34*, 9156.
(33) Zhulina, E.; Birshtein, T.; Pryamitsyn, V.; Klushin, L. *Macromolecules* **1995**, *28*, 5612.

MA011884P